ResearchGate

See discussions, stats, and author profiles for this publication at: https://www.researchgate.net/publication/228373794

Nanoparticles Distribution Control by Polymers: Aggregates versus Nonaggregates

ARTICLE *in* THE JOURNAL OF PHYSICAL CHEMISTRY C · JANUARY 2007

Impact Factor: 4.77 · DOI: 10.1021/jp065635k

CITATIONS
75

READS
26

6 AUTHORS, INCLUDING:

Christophe Déjugnat
Paul Sabatier University - Toulouse III
45 PUBLICATIONS **1,660** CITATIONS
SEE PROFILE

Andrei Susha
City University of Hong Kong
109 PUBLICATIONS **5,312** CITATIONS
SEE PROFILE

Gleb Sukhorukov
Queen Mary, University of London
318 PUBLICATIONS **19,400** CITATIONS
SEE PROFILE

Available from: Christophe Déjugnat
Retrieved on: 02 February 2016

Nanoparticles Distribution Control by Polymers: Aggregates versus Nonaggregates

A. G. Skirtach,*,† C. Déjugnat,†,‡ D. Braun,§ A. S. Susha,§,⊥ A. L. Rogach,§,⊥ and G. B. Sukhorukov▽

Max-Planck Institute for Colloids and Interfaces, Golm/Potsdam D-14424, Germany, Institut de Chimie Séparative de Marcoule, FRE CEA/CNRS 2926, CEA Valrhô BP 17171, 30207 Bagnols sur Cèze Cedex, France, Center for Nanoscience and Photonics and Optoelectronics Group, Physics Department of Ludwig-Maximilians-Universität München, Amalienstr. 54, Munich D-80799, Germany, and Department of Materials, Queen Mary University of London, Mile End Road, E1 4NS London, U.K.

Received: August 30, 2006; In Final Form: September 21, 2006

Aggregation states of both stabilized (by organic ligands) and nonstabilized nanoparticles have been studied in solutions, on plain surfaces, and within the polyelectrolyte multilayer capsules to provide control over formation of aggregates and their uniformity. Adsorption of nanoparticles could be performed either simultaneously with polymers to achieve their uniform (nonclustered or nonaggregated) distribution or without polymers for obtaining nonuniform (clustered or aggregated) distribution. Nanoparticles were characterized; in synthesis of nanoparticles involving gold sulfide the reaction can be stopped at a desired time to control the location of the near-infrared absorption peak. The influence of the uniformity of the nanoparticles distribution on the temperature rise during laser light illumination is numerically calculated; it is shown that the temperature rise on the closely located nanoparticles is higher than on the stand-alone nanoparticles. Further applications of polymer controlled distribution of nanoparticles are anticipated in their self-assembly.

I. Introduction

Research on nanoparticles (NP) is receiving ever-increasing attention. After Mie presented his analysis of scattering from small colloidal particles,[1] the attention to this multidisciplinary area has been continuously growing.[2−6] Development of silver halide photography has been the stimulus behind research on small silver particles.[7] The seminal work by Turkevich[3] provided a simple and reliable method to synthesize colloidal gold NP. Subsequent research in this area was spurred by interest in noble metals,[5] including silver,[8,5] gold,[4,5] and copper[5,9,10] NP. More recently, the interest to metal NP has been growing[11−19] because the burgeoning area of nanotechnology offered new perspectives for developing further applications in molecular sensing[20] and biosensing,[21] molecular imaging,[22] DNA analysis,[23,24] Raman scattering amplification enhancement[25−27] and optoelectronics.[28]

Just as the field of nanotechnology was developing, the terminology has been evolving all along. Indeed, tiny particles were the subject of extensive research but the terms used to describe them were different. For example, in his early work Mie[1] referred to scattering from "small particles". Subsequently, there were "colloidal particles" that received substantial attention.[2] Another term applied to the same particles was "clusters", as in the fundamental study[29] of Kreibig and Vollmer. Recently the term "nanoparticles" has been used more and more often to describe particles in the size range from about 1 nm to 1 μm. The size range between 1 and 100 nm is of particular importance for noble metals especially because the mean free path of electrons (for example, ∼50 nm for gold) lies in this region.

Functionalization of NP surface with organic molecules (also denoted as capping agents, stabilizers, or surface ligands), which usually occurs already at the synthesis stage, provides a large degree of freedom for NP manipulation and use. For example, high affinity of thiol groups to the metal surface can be applied to functionalize NP.[30] On the other hand, nonstabilized (by any organic ligands) NP provide an opportunity of modifying their properties post-preparatively, e.g. by depositing inorganic or organic materials of interest on their surface. That widens the opportunities of surface chemistry modifications, including the possibility of application of such universal methods as layer-by-layer (LbL) deposition.[31−34]

An important area of NP research relates to the condition at which the NP exist—aggregated or nonaggregated state. Control over the NP aggregation is crucially important for many reasons: first and foremost, it is essential to gain control over their aggregation from the point of its prevention and increasing the NP stability; second, a controllable aggregation is significant for applications where the local accumulation of NP is desired; third, NP are increasingly used as sensors in biological applications wherein the aggregation condition determines the sensing mechanism;[19] and finally, optical properties of NP are strongly influenced by aggregation state.[27,35−37] Our current study on nonstabillized NP concentrates on NP obtained by the reaction of Na_2S with $HAuCl_4$ [38−42] due to several reasons. First of all, these particles are truly "nonstabilized" in a sense that they do not carry any organic ligands on their surface; second, they exhibit near-infrared absorption—a desirable parameter for biomedical applications. A somewhat controversial issue[43,44] is that concerning the exact chemical structure of these particular NP (either core−shell structure of so-called "nanoshells"[20,38−40] composed of Au_xS/Au, or aggregates of purely Au NP[41,42]). Identifying the structure of these NP is not directly related to

* To whom correspondence should be addressed. E-mail: andre.skirtach@mpikg-golm.mpg.de. Tel.: +49-(0)-331-567-9235. Fax: +49-(0)-331-567-9202.

† Max-Planck Institute for Colloids and Interfaces.

‡ Institut de Chimie Séparative de Marcoule.

§ Center for Nanoscience, Ludwig-Maximilians-Universität München.

⊥ Photonics and Optoelectronics Group, Ludwig-Maximilians-Universität München.

▽ Queen Mary University of London.

10.1021/jp065635k CCC: $33.50 © xxxx American Chemical Society
Published on Web 12/16/2006 PAGE EST: 9.4

the main subject of the current work but it is shortly discussed here in relation to the aggregation condition of these NP and uniformity of their distribution.

We discuss here the pathways of achieving both uniform (which could also be referred to as nonaggregated) and nonuniform (referred to as aggregated) distributions of NP. The focus of current study is on achieving a controllable distribution of NP by using charged polyelectrolyte polymers. The results of controlled adsorption of metal NP on polyelectrolyte multilayer capsules[45] for both nonstabilized and stabilized NP are presented. Stabilization is referred to as the existence of a stabilizing ligand or a surfactant on the surface of NP. It is demonstrated that both uniform and nonuniform distributions of NP can be achieved on polyelectrolyte multilayer surfaces depending on their premixing with polymers. The uniform distribution of NP is defined as that without clusters or aggregates of NP on the surface of the capsules, whereas the nonuniform distribution is referred to as that with clusters of NP or their aggregates. Control over the distribution of NP and their adsorption is performed by controlling their interaction with polymers. Our study focuses on nonstabilized NP (nsNP) where the polymers interact directly with NP. We compare these results with the case of stabilized NP (sNP) wherein the added polymer interacts with the stabilizing agent thus affecting their adsorption. For these two types of NP it is possible to achieve either uniform or nonuniform distribution, although the conditions for their adsorption are different.

The distribution of metal NP is also significant for remote release from microcapsules[46−50]—the unique system for delivery of encapsulated materials into designated compartments. The microcapsules are fabricated by the LbL deposition method[31−34] by alternately adsorbing oppositely charged polymers on colloidal templates.[45] Such a method allows for control over the surface buildup of the capsules. Encapsulation of polymers and other materials can be achieved, for example, by pH-controlled swelling and shrinking of capsules.[51,52] In the area of biomedical applications, polyelectrolyte multilayer capsules can be used for delivery of the encapsulated materials into biological cells[53,54] and serve as fluorescence markers for cell sorting.[55] In regard to remote release of encapsulated materials, the influence of nonuniformity of the NP distribution, particularly of clusters or aggregates, is of significant importance for optimizing the conditions for release from the polyelectrolyte multilayer capsules. In general, the idea of remote release of encapsulated materials is based on affecting the outer shell comprised of polymer layers by, for example, laser light. Energy absorbed by NP incorporated into the capsule walls is converted into thermal energy and is sufficient to rupture the polymer network constituting the walls of the capsules. The real time release of encapsulated polymers was demonstrated on a single capsule level;[49] it was also shown that such parameters as the surface filling factor or the surface density of metal NP on the capsules, together with size and absorption of NP, influence the efficiency of them as light absorbing centers.[49]

In general, it is desirable to control the distribution[56−58] of NP for numerous applications. In some more specific examples, the uniform/nonaggregated distribution of NP is of interest for their self-assembly on planar surfaces,[59−64] while the nonuniform/clustered type is better suited for remote release applications.[46−50]

II. Methods and Experimental Section

2.1. Materials. Negatively charged polyelectrolyte poly(sodium 4-styrenesulfonate) (PSS), ~70 kDa, and positively charged polyelectrolyte poly(allylamine hydrochloride) (PAH), ~70 kDa, were purchased from Sigma-Aldrich (Germany). Inorganic acids, bases, salts, and tetrahydrofuran (THF) were obtained from Roth (Germany). Monodisperse polystyrene (PS) latex particles (10.25 μm in diameter) were obtained from Microparticles GmbH (Germany) as 10% w/w aqueous suspensions. Water used in all experiments was prepared in a three-stage Millipore Milli-Q Plus 185 purification system and had a resistivity higher than 18.2 MΩ·cm^{-1}.

2.2. Nanoparticles. Two types of NP, in regard to their stabilization by organic ligands, were examined in this study: nonstabilized and stabilized; stabilization is referred to as functionalization or decoration of the surface with organic ligands. Gold NP stabilized by 4-(dimethylamino)pyridine (DMAP) were prepared according to the previously published method[65] and are abbreviated as sNP (stabilized nanoparticles) throughout this article. The sNP were relatively monodisperse with the mean diameter of 8 nm, and aqueous suspensions were obtained at a concentration of 3×10^{14} NP/mL.

Nonstabilized nanoparticles (nsNP) are referred to as such since they do not initially contain any stabilizing organic ligands or surfactants attached to their surface. The overall stability of the aqueous suspension containing these nsNP is attributed to the double layer of inorganic ions on the NP surface. The presence of these ions originates from the synthetic conditions; they make the NP negatively charged and prevent them from spontaneous aggregation. These NP, assigned to either gold sulfide/gold core−shell NP (also denoted as nanoshells)[39,40] or aggregates of gold NP,[41,42] were prepared by a two-step reaction of Na_2S with $HAuCl_4$.[38] In a typical synthesis, 10 mL of 1 mM Na_2S solution was added to 10 mL of 2 mM $HAuCl_4$ solution followed by stirring for 5 min and addition of 5 mL of 1 mM Na_2S solution. Two-step addition of Na_2S solution was found to provide a better spectral quality of resulting NP than the one-step addition of the full Na_2S amount. The reaction can be stopped at any stage by injection of an additional amount of 1 mM Na_2S (1:1 to the reaction volume). This addition allowed us to obtain NP solutions with a fixed position of absorption peak. They were stable for months and showed no or negligible changes in their absorption spectra.

2.3. Methods of Preparation of Polyelectrolyte Multilayer Capsules with Nanoparticles. Polyelectrolyte multilayers were assembled on PS latexes by the layer-by-layer deposition technique,[31−34] using positively charged PAH (1 or 5 mg/mL) and negatively charged PSS (2 mg/mL or 5 mg/mL) solutions containing 0.5 M NaCl. For each experiment, 300 μL of the commercial PS cores suspension was used, corresponding to approximately 5×10^7 cores. Each adsorption step was conducted using 1 mL of the polyelectrolyte solution for 12 min, followed by 3 washes with pure water. Each time the (coated) PS cores were separated from the supernatant by centrifugation (1 min at 1000*g*). Finally, the dissolution of the cores was achieved using THF according to the previously described procedure.[50] Subsequent washing with water resulted in hollow polyelectrolyte microcapsules in aqueous suspensions.

2.3.a. Method A (Adsorbing NP Apart from Polymers). NP were adsorbed between the polyelectrolyte multilayers. Typically, the PS cores were first coated with one or several (PAH/PSS) bilayers. Then they were incubated during 2 min with the aqueous suspension of sNP. After it was washed with water, the multilayer assembly was completed with several (PAH/PSS) bilayers. Using this method, two types of microcapsules were prepared, containing either one layer of sNP in the middle of the polyelectrolyte film or one layer with sNP for every polyelectrolyte bilayer. For 12 layers, the structures

are $(PAH/PSS)_3$sNP$(PAH/PSS)_3$ or $(PAH/sNP/PSS)_6$, respectively. Since by using this method all NP are adsorbed on the polymeric film, the amount of introduced NP could be controlled by varying either the concentration or the volume of the aqueous suspension of NP.

In the case of nsNP the deposition was the same with a subtle difference that the addition of one more layer of PSS after NP $(PAH/PSS)_3$nsNP/PSS$(PAH/PSS)_3$ helps to reduce aggregation of capsules. Note that the NP were adsorbed onto a polyelectrolyte layer with opposite charge; for example, negative nsNP nanoparticles were adsorbed on PAH whereas positively charged sNP were adsorbed on PSS.

2.3.b. Method B (Premixing Nanoparticles with Polymers). sNP were first premixed with a polyelectrolyte solution. Then this mixture was used as a dipping solution during the LbL deposition. Typically, 250 μL of NP suspension was premixed with 1 mL of polyelectrolyte solution. For example, mixing 250 μL of sNP (3×10^{14} particles/mL) with 1 mL of PAH (5 mg/mL in NaCl 0.5 M) led to the final PAH-sNP solution containing 4 mg/mL PAH, 6×10^{13} particles/mL sNP and 0.4 M NaCl.

In the case of nsNP, they were premixed with PAH (in the same proportions) so the same salt concentration (0.4 M NaCl) was obtained after premixing.

This mixture was then used as the "doped" polyelectrolyte solution during the LbL process with a typical incubation time of 12 min.

2.4. Experimental Techniques. Optical images of polyelectrolyte capsules in solution were obtained on a Leica TCS SP confocal scanning microscope (Leica, Germany) equipped with a 100×/1.4−0.7-oil immersion objective. CARY 50 Conc. UV−vis spectrometer (Varian, Germany) was used for absorption spectra measurements. Dynamic light scattering (DLS, Malvern Instruments, U.K.) system, analytical ultracentrifugation (MPI-KG, Germany), and TEM (Zeiss EM 912 Omega) were used for characterization of NP and their aggregates. The capsules were investigated by TEM in the dry state: typically a tiny amount of the solution containing the microcapsules was dried on a carbon film coated copper grid.

III−IV. Results and Discussion

3. Synthesis and Characterization of nsNP. As it was mentioned earlier, the nsNP used in this study were synthesized by reaction of Na_2S with $HAuCl_4$. Depending on the synthetic conditions, like reagent ratio and even the aging time of sodium sulfide, this reaction can proceed to different stages. For example, the addition of a low amount of sulfide to gold(III) salt leads to turbid yellow solutions because of the formation of pure sulfur. If a large excess amount of sodium sulfide is added, all the gold(III) ions are bonded to Au(III) sulfide. Other oxidation states of Au, in a form of AuS, Au_2S_2, or Au_2S are also possible, in the course of red-ox reactions taking place.[66,67] The absorption spectrum of gold sulfide corresponds to spectra marked by "0" in Figure 1a,b. We note that TEM studies conducted at this stage already indicate the presence of crystalline particles in the solution.

In the presence of free Au(III) ions in solution, the reduction of gold sulfide(s) to metal gold proceeds according to the following reaction:[66]

$$Au_2S_3 + 6AuCl_3 + 12H_2O \rightarrow 8Au + 3H_2SO_4 + 18HCl \quad (1)$$

It is important to point out that if comparable molar amounts of sulfide ions and Au(III) salt are used (S/Au in the range 1:1 to 1:2.5), two scenarios for reaction 1 are possible. In the first case, the reaction proceeds to the end product of Au NP involving all of the existing Au_xS NP in the solution. Absorption spectrum of this solution shows a single peak at 520 nm (data not shown). In the second case, the reaction product is characterized by two peaks in its absorption spectrum: one at 520 nm (Au NP) and another in the near-infrared, Figure 1. The nature of the latter peak was discussed controversially in the literature, being ascribed either to so-called nanoshells consisting of Au_xS core and Au shell,[38−40] or to the gold nanoparticle aggregates.[41,42] An interesting feature of this reaction is that the addition of excess of sodium sulfide, which binds all the remaining Au(III) ions still present in the solution, can be used to stop the reaction at a desired time.

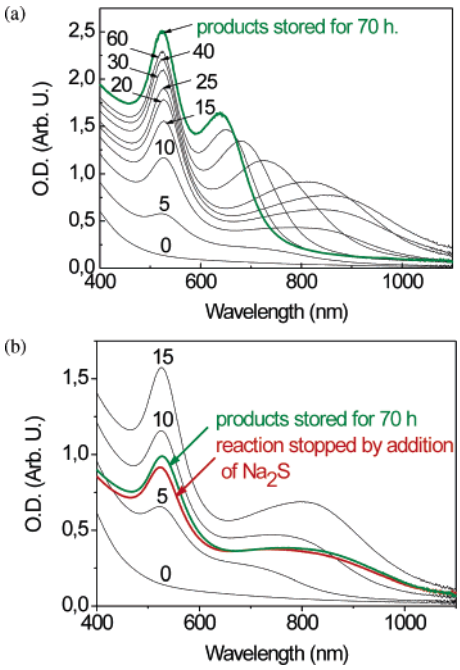

Figure 1. UV−vis absorption spectra of nsNP. (a) Temporal changes for the sample when the proceeding reaction, eq 1, is not stopped. (b) Temporal changes for the sample when the proceeding reaction, eq 1, is stopped by adding the excess of Na_2S. The corresponding time, in minutes, elapsed from the moment of reagents mixing is indicated next to the corresponding curve. After the reaction is stopped, the stored products were measured after 70 h.

Using the possibility to stop reaction 1, two kinds of samples were prepared. In the first case (no extra sodium sulfide added), the reaction proceeded for a long time with continuous changes of the absorption spectrum, including the increase of the absorption peak at 520 nm and a blue shift of the second, infrared peak, taking place (Figure 1a). These spectral changes came to saturation after approximately 70 h, and no more spectral changes were observed even after months of storage. The NP obtained so far were referred to as nsNP-1 further in text. In the second case, the addition of excess of sodium sulfide (which binds all the remaining Au(III) ions present in the solution) has been used to stop reaction 1 in 15 min. This led to the conservation of positions of both absorption peaks (Figure 1b). These NP are referred to as nsNP-2. Stopping the reaction by adding sodium sulfide for controlling the location of the near-infrared absorption peak has not been reported in the literature to the best of our knowledge.

We have further analyzed the size distribution of nsNP-1. The size distribution measured by dynamic light scattering (DLS) showed existence of NP with sizes between 20 and 120 nm, Figure 2 (green bars). In addition, we have performed the size characterization of the same sample by analytical ultra-

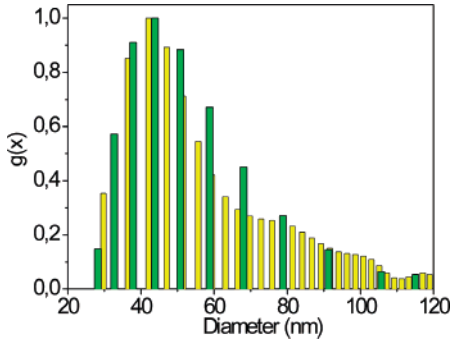

Figure 2. Dynamic light scattering (green bars) and ultracentrifugation (yellow bars) measurement data for nsNP-1 sample.

centrifugation. This technique[68,69] monitors sedimentation of NP at a specific absorption wavelength; therefore the contribution to absorption at this wavelength of NP of specific size can be extracted. When monitored at 750 nm the size distribution measured by ultracentrifugation, Figure 2 (yellow bars), was found in agreement with the data obtained by DLS, Figure 2 (green bars). Gold NP of larger sizes result in the red-shift (from 520 nm) of the surface plasmon resonance,[70] but such size distribution does not explain the appearance of the second absorption peak in the near-infrared.[70] The nature of absorption peak in the near-infrared is still controversial as reported in the literature.[43,44] It was claimed that these NP are core−shell structures composed of Au_xS/Au,[39] formed in the course of formation of metal gold at the surface of preformed Au_xS NP. Yet, the analytical data of surface characterization of these NP did not support the core−shell structure[40] pointing to their purely metallic nature and assigning the peak in the near-infrared to gold aggregates.[41,42] Spectroscopic studies on single NP supported, in turn, the core−shell model.[20,44] The main goals of this work, the controlled distribution of NP by polymers, are not associated with confirming or refuting these controversial issues, and therefore no direct arguments toward any of the sides are provided. However, the data obtained by characterizing the uniform distribution argue against the assignment of near-infrared absorption peak to aggregates of purely gold NP since it is demonstrated that even when the formation of NP aggregates is prevented, by forming their uniform distribution through the addition of polymers, the peak in the near-infrared part for these nonaggregated NP still exists. These results can be seen in Figure 3 which presents TEM images of nsNP deposited on the copper grid and UV−vis absorption spectra in the solution of NP before depositing them on the TEM grid for two cases: with and without the addition of polymers. It can be seen from this figure that the peak in the near-infrared part of the spectrum exists for the original solution of nsNP-1, and when they were deposited on the TEM grid, the aggregates were formed, Figure 3a. When positively charged polymers (PAH) were added to the solution of these NP, Figure 3b, the peak in the near-infrared part of the spectrum still existed but the distribution of the NP on TEM grid was clearly nonaggregated, Figure 3b. We note that although most NP were found in the nonaggregated form, some small aggregates could still be found even after the addition of the polymers. One such example is shown in the inset to Figure 3b. The number of such aggregates is small but that suggests that particles binding through sulfur species on the NP surfaces to each other could occur.[27] Similar experimental data were found for nsNP-2, Figure 3c,d.

Further we have investigated the influence of negatively (PSS) or positively (PAH) charged polyelectrolytes on the stability of nsNP solutions by monitoring ζ- potential. The experiment has been done according to the method illustrated in Figure 4. Upon mixing of negatively charged nsNP (ζ-potential in water −47 mV) with negatively charged PSS, precipitation of NP took place (Figure 4). Upon mixing of nsNP with positively charged PAH, the solution remained stable and transparent, and the ζ-potential of NP mixed with PAH (and then washed with water) changed to the value of +51 mV. The reversal of charge clearly indicates adsorption of PAH onto nsNP. Thus, positively charged polymer chains interact with negatively charged nsNP and thus act as the stabilizing agent. We note that such coating of NP with polymers is similar to the results presented by other groups.[71,72]

4. Preparation and Characterization of Microcapsules. 4.1. Microcapsules with Stabilized Nanoparticles. 4.1.a. Stabilized Nanoparticles on Microcapsules with Nonuniform Distribution. Using Method A, the precoated PS cores were mixed directly with the aqueous suspension of sNP. As these particles are positively charged, they were adsorbed on films presenting PSS as the outermost layer. This method was used to introduce from one up to six sNP layers in the multilayers. After dissolution of the core, hollow capsules were obtained from $(PAH/PSS)_3sNP(PAH/PSS)_3$ to $(PAH/PSS/sNP)_6$. For each experiment, all the NP initially put in contact with the coated PS cores were adsorbed onto the preceding layers. The adsorption process was very fast, and incubation time of 1 min was enough to ensure complete adsorption, as monitored by UV−vis spectroscopy: after incubation and centrifugation, the supernatants were always clear and did not present any sign of the presence of sNP.

This method enables adjustment of the concentration of deposited NP by varying either the volume or the concentration of the dipping solution. We note that the concentration can also be adjusted by varying the number of NP layers. The scheme of method for nonuniform distribution of NP is shown in Figure 5a. A typical TEM image of the surface of a capsule and confocal microscope image of hollow capsules in water are presented in parts b and c of Figure 5, respectively.

Using optical microscopy in transmission mode, the NP-containing capsules appear darker than purely polymer $(PAH/PSS)_n$ capsules, due to the presence of adsorbed sNP (Figure 5c); the apparent homogeneous coverage indicates that no aggregates of several hundreds of nanometers were formed. However, TEM observations, Figure 5b, clearly indicate the nonuniform distribution of NP, with the formation of aggregates with size ranging from 20 up to 150 nm. There are areas of high concentration of sNP together with areas of low concentration. Although Method A can be used to control precisely the amount of sNP in the polyelectrolyte multilayers, it always led to the nonuniform distribution of these NP. The aggregation may be due to a very fast adsorption, essentially driven by attractive electrostatic interactions between positively charged sNP and negatively charged PSS-coated surfaces, Figure 5a.

4.1.b. Stabilized Nanoparticles on Microcapsules with Uniform Distribution. In the method described above, there is no mechanism for influencing the interaction of the NP with the polyelectrolyte surface. It is possible to induce the competition between the charges of the sNP by premixing them with identically charged polyelectrolyte. In Method B, sNP suspension was first mixed with PAH solution before adsorption onto the PS (coated) cores. PAH was chosen because it has the same charge as NP stabilized with DMAP, while PSS would have led to the formation of complexes and aggregates already in solution. UV−vis absorption measurements showed that the

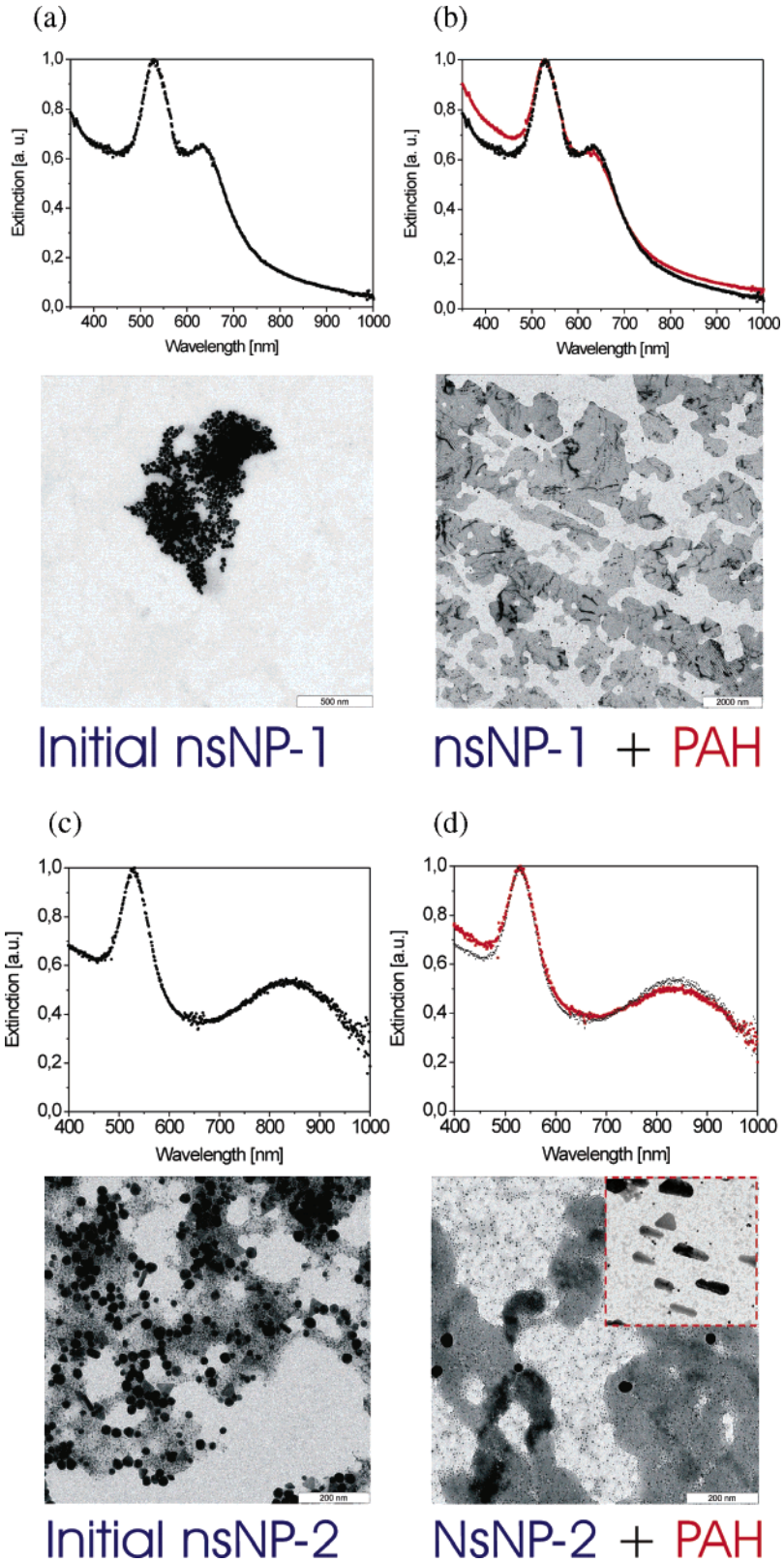

Figure 3. (a) UV−vis absorption measurement of nsNP-1 and their TEM image. (b) UV−vis absorption measurement of nsNP-1 mixed with polymers (PAH) and the corresponding TEM image. Parts c and d present similar results for nsNP-2.

spectrum of the mixture (PAH and sNP) is almost identical to that of sNP (λ_{max} = 518 nm). This indicates that there is no interaction between the positively charged sNP and PAH. Here, the presence of salt (0.4 M NaCl) screens electrostatic interactions, and the pH of the solution is low enough (between 4 and 6.5, depending on PAH and sNP concentrations) to ensure complete protonation of the PAH. As a result, this mixture corresponds to a mixture of sNP with a strong polycation exhibiting no significant interaction.

Microcapsules prepared using Method B had the following composition (PAH-sNP/PSS)$_6$. Different samples were prepared by varying either the PAH concentration (1 or 5 mg/mL in the presence of NaCl 0.5 M) or the concentration of NP (from 3 × 10^{13} to 3 × 10^{14} nanoparticles/mL) of the solutions to be mixed.

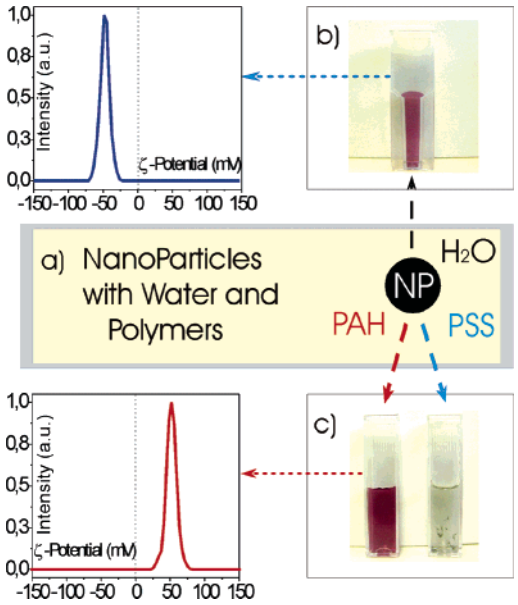

Figure 4. (a) Scheme for studying the interactions of nsNP with oppositely charged polyelectrolytes. (b) Photograph of nsNP in water; ζ-potential measurement is shown to the left of the photograph. (c) Photographs of nsNP mixed with PAH (left) and PSS (right). ζ-potential measurement on nsNP mixed with PAH is shown to the left of the photograph. The concentration of the polymers was 5 mg/mL in 0.5 M NaCl in both cases.

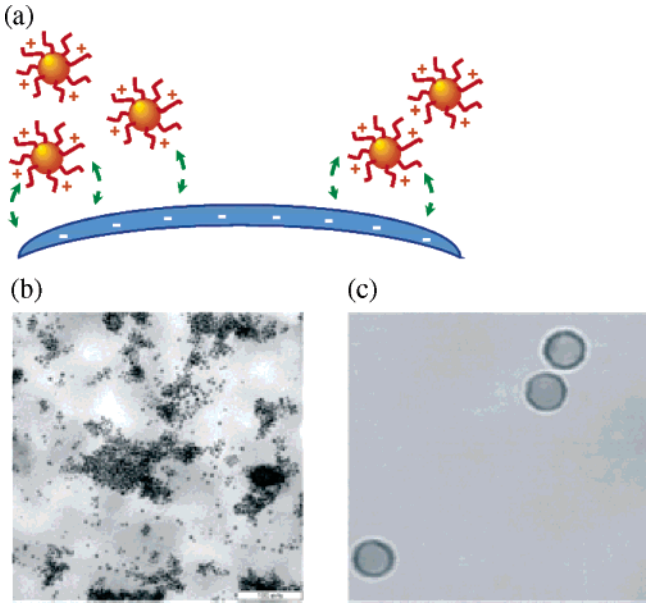

Figure 5. (a) Schematics of obtaining the *nonuniform* distribution of sNP on polyelectrolyte multilayer capsules. (b) TEM image of the *nonuniform* distribution of sNP on microcapsules. (c) Confocal microscope image of the capsules with *nonuniform* distribution of sNP.

In all cases, after incubation of the cores with the mixtures during 12 min, the supernatants were colored, and UV−vis absorption measurements confirmed that only a part of the sNP was adsorbed to the cores while the rest was not adsorbed and remained free in the supernatant. These observations support the idea of competition between positively charged PAH and sNP toward the electrostatic adsorption onto the negative PSS surface, Figure 6a. Although the presence of a large excess of PAH could have led to a confinement of sNP by pushing them together, no aggregation occurred and this shows the efficiency of the stabilization by DMAP.

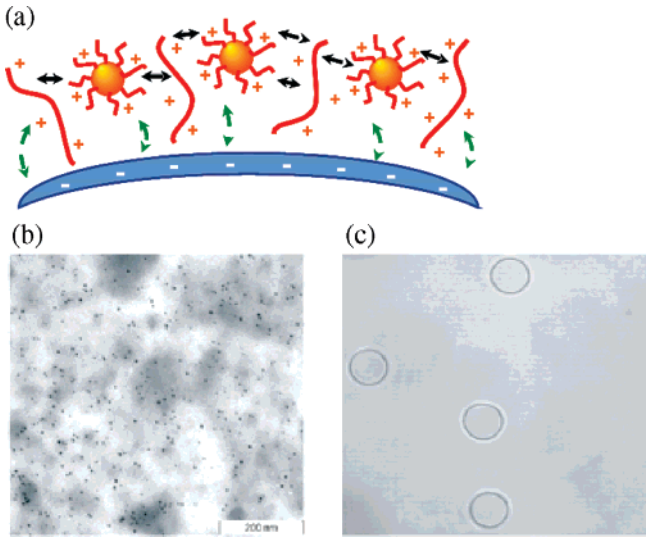

Figure 6. (a) Schematics of obtaining the *uniform* distribution of sNP on polyelectrolyte multilayer capsules. (b) TEM image of the *uniform* distribution of sNP on microcapsules. (c) Confocal microscope image of the capsules with *uniform* distribution of sNP.

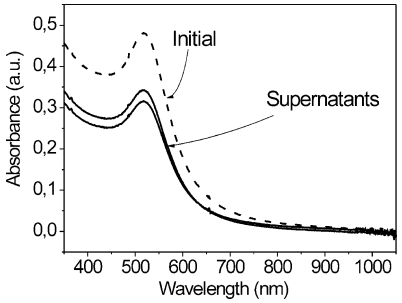

Figure 7. UV−vis absorption spectra of supernatants after deposition of sNP-PAH premixed solution. The dashed line represents the spectrum of the initial solution. The solid lines below show the spectra of two supernatants after the adsorption; the spectra of all other supernatants are located between these two curves.

The scheme of adsorption of NP with uniform distribution is shown in Figure 6a. Here the competition between the charged groups on sNP and the polymers in the solution is the driving mechanism of the adsorption. Typical TEM images are presented in Figure 6b. The striking difference between the distributions of sNP prepared using Method A, Figure 5b, or Method B, Figure 6b, is obvious. In the latter case, the deposition of the NP occurred in a uniform way. Confocal microscope observation of $(PAH\text{-}sNP/PSS)_6$ hollow microcapsules showed that the capsules appeared homogeneous with a slight gray tinge, Figure 6c; the darkness depends on the sNP concentration. The result of the electrostatic repulsions between positively charged DMAP on sNP and PAH is that these moieties are pushed away from each other producing a uniform competitive adsorption of the sNP on the templates. Moreover, due to the competition between charges, not all of the NP were adsorbed on the capsules. For a given concentration of these NP, no significant difference was observed in the presence of 0.5 M NaCl either using 1 or 5 mg/mL of PAH. Even for the lower concentration, PAH is still in large excess compared to the NP, and its competition with sNP is not enhanced by increasing the concentration.

By analyzing the supernatants with UV−vis absorption data, the amount of adsorbed NP was measured as a function of the initial concentration, Figure 7. For each fixed concentration, the absorption of sNP in the presence of PAH was constant and independent of the position of this layer in the film, except

TABLE 1: Adsorption of Stabilized Gold NP in the Presence of PAH (Method B), for One Deposition Step[a]

intit. concd stabilized NP (NP/mL)	concd. after mix. with PAH (NP/mL)	% adsorbed (from UV−vis)	number adsorbed NP	surface density (NP/μm^2)	surface filling factor, F_S
3×10^{13}	6×10^{12}	69	5.3×10^{12}	314	0.10
6×10^{13}	12×10^{12}	39	5.9×10^{12}	350	0.11
15×10^{13}	30×10^{12}	29	10.9×10^{12}	651	0.22

[a] PSS was the outermost layer on the coated PS templates.

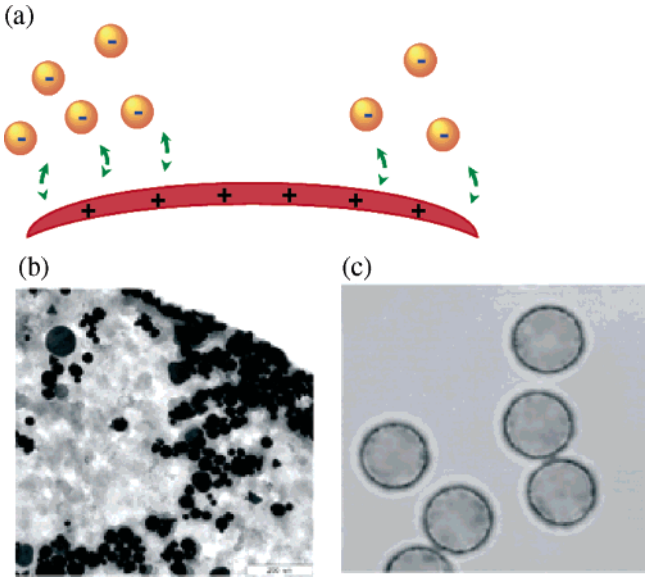

Figure 8. (a) Schematics of obtaining the *nonuniform* distribution of nsNP on polyelectrolyte multilayer capsules. (b) TEM image of the *nonuniform* distribution of nsNP on microcapsules. (c) Confocal microscope image of the capsules with *nonuniform* distribution of nsNP.

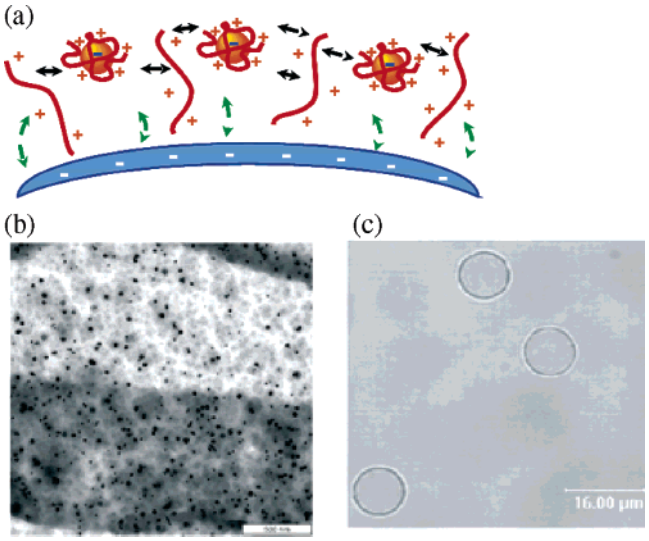

Figure 9. (a) Schematics of obtaining the *uniform* distribution of nsNP on polyelectrolyte multilayer capsules. (b) TEM image of the *uniform* distribution of nsNP on microcapsules. (c) Confocal microscope image of the capsules with *uniform* distribution of nsNP.

for the very first deposition on the "naked" PS cores. In this latter case, the amount of adsorbed NP was observed lower than that when adsorbed on PSS layer. This indicates that the interaction between sNP and PS is weaker than the interaction between them and the strong polyanion PSS. The results presented in Table 1 correspond to the adsorption of sNP from a PAH−Au mixture at different concentrations. For each concentration, the same amount of NP was adsorbed, showing that there is no influence of the previously adsorbed layers and therefore no significant diffusion of sNP through the deposited film for each deposition step. The amount of adsorbed sNP increases with increasing the concentration, but this dependence is not linear. From these values one can calculate the surface density of the NP, F_S, defined as the ratio of the surface area covered by NP to the total surface area of the capsule.[49] These calculated parameters represent the upper limits assuming that there was no significant loss of the templates during LbL assembly.

4.2. Microcapsules with Nonstabilized Nanoparticles. 4.2.a. Nonstabilized Nanoparticles on Microcapsules with Nonuniform Distribution. Using Method A, the precoated PS cores were mixed directly with the suspension of nsNP, Figure 8a. Since these particles are negatively charged, they were adsorbed on films possessing PAH as the outermost layer. For each step, all NP were adsorbed onto the PS cores. The amount of nsNP within the polyelectrolyte multilayers can therefore be tuned, like in the case of sNP, by varying the concentration of NP and/or the number of adsorbed layers. Similarly to that with sNP, a very nonuniform distribution of the nsNP was observed, Figure 8b. Due to the bigger size of the formed aggregates, the capsules appeared already inhomogeneous, as evidenced in confocal micrograph, Figure 8c, and this can also be clearly seen by TEM, Figure 8b. The nonuniform distribution does not allow one to conclude whether the nsNP were nonaggregated before adsorption on the capsules. Alternatively, the uniform distribution of nsNP can be achieved by using the competition between the charges on the NP and added polymers, as described in the following section.

4.2.b. Nonstabilized Nanoparticles on Microcapsules with Uniform Distribution. Premixing the negative nsNP with the oppositely charged polyelectrolytes, PAH (5 mg/mL in 0.5 M NaCl), resulted in forming stable suspensions. No change of color in the solution was visually observed, and no spectral changes were detected. The scheme of premixing of nsNP with PAH is shown in Figure 9a. It can be seen from this figure that the polyelectrolytes both stabilized the NP and pushed them apart upon the adsorption. This resulted in formation of nonaggregated, uniform distributions of nsNP on the capsules, Figure 9b. Figure 9b shows that NP are deposited in the nonaggregated state; the resulting microcapsules can be seen in Figure 9c.

The mechanism of formation of uniform distribution with nsNP is similar to that in the case of sNP. Indeed, in the case of sNP the positively charged DMAP is repelled from positively charged PAH, pushing the NP apart. In the case of nsNP, some positively charged PAH is adsorbed on the NP while the rest of the polymer pushes them apart upon adsorption. The two cases are similar since PAH was in excess.

We note that if premixing of negatively charged nsNP was carried out with negatively charged polymers, PSS, then aggregated, nonuniform distributions were formed. This is consistent with the results presented in Figure 4.

V. Heating of Nanoparticles: A Theoretical Study

5. Why Controlling the Distribution of Nanoparticles Is Needed. Control over the distribution of NP is of interest for a variety of applications.[19,26,27,59−64,73] One of the applications requiring control over the distribution of NP is the release of encapsulated materials from microcapsules.[46−50] It is based on the interaction of laser or other energy source with NP. The latter absorb energy and heat up resulting in the rupture of the polymer shell and releasing encapsulated materials. It is essential to note that the NP heat up the surrounding environment locally, which results in high local gradient of heat but only moderate heating in the whole volume of solution around microcapsules.[11] In this application, if the NP are located in close proximity to each other, the heat emission processes add up. Or alternatively, if the NP are sparsely distributed, the heating effects from neighboring NP do not add up. We note that optimization of the heating of NP can be conducted using the physical parameters.[74] So once the physical parameters of NP are optimized,[74] it is their distribution that will determine the optimum conditions. The experimental data presented above demonstrate how to obtain the desired distribution, while the analysis provided in this section shows the extent of the influence of the distribution of NP on the temperature rise in the vicinity of NP.

To assess the influence of the distribution of the NP we have calculated the temperature rise on the NP for their uniform and nonuniform distributions. The temperature at the center of a metal nanoparticle can be defined as follows:[49,75,76]

$$T = \frac{r_0^2 E}{K_m} \tag{2}$$

$$E \approx E_0\left(\frac{1}{3} + \frac{2b_2}{\pi}\int_0^\infty \frac{e^{-y^2\tau}}{y}\frac{(\sin y - y\cos y)dy}{(c\sin y - y\cos y)^2 + (b_1 y \sin y)^2}\right) \tag{3}$$

where r_0 is the radius of nanoparticle, K_{NP} and K_M are thermal conductivities of metal and surrounding medium, respectively, $b_i = (K_M/K_{NP})^i(k_m/k_{np})^{0.5}$, $i = 1$ or 2, k_{np} and k_m are thermal diffusivities of nanoparticle and the medium, respectively, $\tau = tk_{np}/r_0^2$, and t is time; also, this expression does not include convection and dissipation. From the last expression it can be seen that the time scale of the thermal processes is described by the characteristic diffusion time, which, for NP with radius 5−20 nm and $k_{np} = K_{NP}/\rho_{Au}C_{Au} = 1.4 \times 10^{-4}$ m^2 s (with K_{NP} = 314 W/mK (Au)), can be estimated as $t_{Au} \sim 1/(k_{np}/r_0^2) \sim 2-8 \times 10^{-12}$ s $\sim$ 1 ps.

Temperature on NP can be calculated knowing E_0, which is proportional to incident intensity, and absorption coefficient, which (for $r_0 \ll 2\pi/\lambda$) can be written as follows:[29]

$$Q_{abs} \approx \frac{4\pi r_0}{\lambda} Im\left(\frac{m^2 - 1}{m^2 + 2}\right) \tag{4}$$

where m is the complex refractive index and λ is the wavelength of light. Numerical analysis of the temperature distribution on the capsule was performed with the finite element simulator Comsol Femlab. The physical parameters of the materials were as follows: water density $\rho = 1000$ kg m^{-3}, heat capacity C_p = 4200 J kg^{-1} K^{-1}, heat conductivity K_w= 0.54 W m^{-1} K^{-1}, heat conductivity of the surrounding medium can be estimated $K_M \sim 0.3-0.4$ W/mK.[77] Our simulations are accurate since they were verified experimentally,[49] and the measurements are based on the earlier reported technique.[78,79]

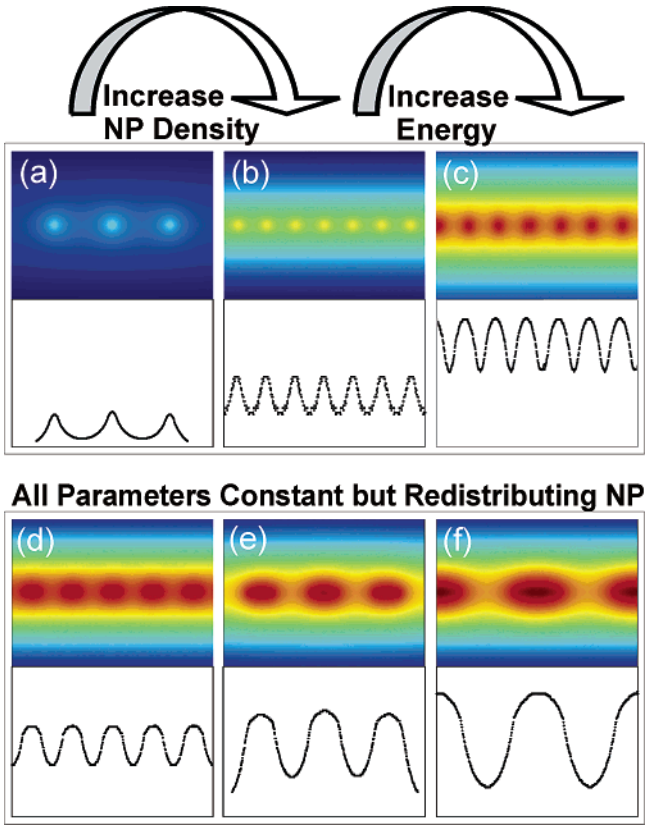

Figure 10. (a−c) 2-D temperature calculations upon heating for uniform distribution of NP. For uniform distribution higher temperature rise can be induced either by higher density of NP (b) or by higher supplied energy/intensity (c). The temperature rise for nonuniform distribution (d−f) shows that higher increases on NP can be induced by their denser location, i.e., aggregated distribution.

The temperature distribution for the uniform distribution of NP is shown in the upper row of Figure 10a−c, while the latter case (nonuniform distribution) is shown in the bottom row of Figure 10d−f. It can be seen from Figure 10a−c that the temperature rise can be increased either by increasing the concentration of NP, Figure 10b, or by raising the supplied energy, Figure 10c. In both cases the temperature rise will be distributed throughout the layer or layers containing the NP. In the case of nonuniform distribution of NP, the temperature increase is located locally on the clustered NP, Figure 10d−f. Here the number of NP was kept constant but their position was changed from uniform to the nonuniform. The average temperature of the layer does not change appreciably but the temperature rise on NP is substantially higher on the clusters of 2, 3, and 4 NP, parts d, e, and f of Figure 10, respectively. It can be also noted that the temperature in the "valleys" of the temperature distribution profiles—the areas between the clustered NP in Figure 10d−f—is lower but the peaks are higher, Figure 10d−f. This is the fundamental difference between the uniform and nonuniform distribution of NP. Therefore, if NP are located in a cluster the temperature increases will be concentrated closely to this area leaving the bulk of the surface unaffected. Furthermore, the clusters of NP can increase the temperature by 30%, Figure 11a, which is achieved with the same concentration of NP and the same energy but just distributing the NP nonuniformly. Therefore, positioning the NP or their distribution plays a crucial role in heating of NP. We also note that the temperature rise is a linear function of the supplied energy, Figure 11b. The supplied energy and absorption of NP are the parameters that play an important role in the temperature rise

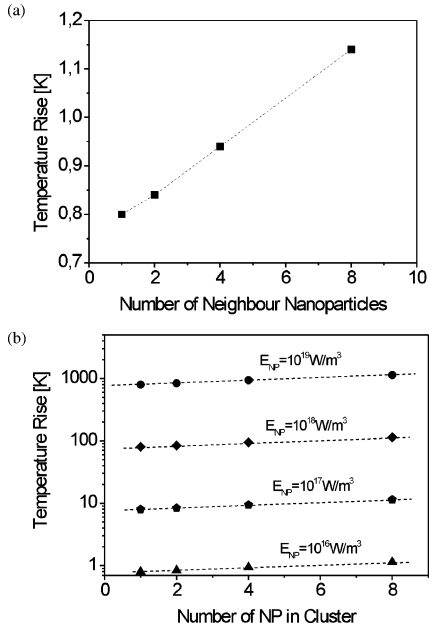

Figure 11. (a) Relative temperature rise as a function of the number of neighbor NP at the energy density 10^{16} W/m^3. (b) Temperature rise as a function of the number of nearest neighbor NP plotted at various values of energy, E_{NP}, on NP.

on NP. The former can be adjusted by the emitting energy source (for example, laser), while the latter can be tuned by choosing either uniform distribution, Method A, or nonuniform, Method B, distributions described in this study.

VI. Conclusions

In conclusion, both uniform and nonuniform distributions of stabilized and nonstabilized NP were obtained upon their adsorption in the presence of polymers on planar supports and on polyelectrolyte multilayer capsules. The uniform (also referred to as nonclustered or nonaggregated) distribution resulted when NP were adsorbed together with the polymers, while the nonuniform distribution (also referred to as clustered or aggregated) was obtained when NP were adsorbed separately from the polymers. For nonstabilized NP obtained by the reaction of Na_2S with $HAuCl_4$, the absorption peak in the near-infrared exists even when the formation of NP aggregates was prevented by addition of polymers; that does not support the assignment of this peak to the aggregates of gold NP.[41,42] The reaction of Na_2S with $HAuCl_4$ can be stopped at a desired time by adding excess of sodium sulfide; this process can be used to control the location of the absorption peak in the near-infrared part of the spectrum.

Control over the distribution of NP is of significant interest to numerous applications, for example, to release encapsulated materials from capsules, where NP are used as energy absorbing centers for raising the temperature and increasing the permeability of the shells for the release. It was found by numerical simulations of the temperature that the nonuniform distribution of NP creates higher local temperature increases on NP and lower local increases in the areas without NP than those obtained with their uniform distribution. Thus, nonuniform distribution creates highly local temperature rises and therefore represents a more efficient NP allocation for remote release from capsules. We also note that controlling the distribution of NP and their arrays by polymers is of interest to self-assembly.

Acknowledgment. We gratefully acknowledge Prof. H. Möhwald for stimulating discussions and support throughout this research. We also thank R. Pitschke for TEM imaging, H. Zastrow for DLS, and Dr. H. Cölfen and A. Völkel for ultracentrifugation measurements. The support by the 6th FP EU-project STREP-NMP3-CT-2005-516922 "SelectNANO", the Volkswagen Foundation (I/80 051-054), and the 6th FP EU-project STREP-001428 "NANOCAPS: Nanocapsules for targeted delivery of chemicals" is kindly acknowledged. D.B. thanks the Emmy Noether Program of the Deutsche Forschungsgemeinschaft for support.

References and Notes

(1) Mie, G. *Ann. Phys.* **1908**, *25*, *377*.
(2) Gans, R. *Ann. Phys.* **1915**, *47*, *270*.
(3) Turkevich, J.; Stevenson, P. C.; Hillier, J. *Discuss. Faraday Soc.* **1951**, *11*, *55*.
(4) Doremus, R. H. *J. Chem. Phys.* **1964**, *40*, *2389*.
(5) Johnson, P. B.; Christy, R. W. *Phys. Rev. B* **1972**, *6*, *4370*.
(6) Henglein, A. *J. Phys. Chem.* **1993**, *97*, 5457.
(7) Berry, C. R.; Skillman, D. C. *J. Photogr. Sci. Eng.* **1969**, *17*, 145.
(8) Klein, E.; Metz, H. *J. Photogr. Sci. Eng.* **1961**, *5*, 5.
(9) Doremus, R.; Kao S. C.; Garcia R. *Appl. Opt.* **1992**, *31*, *5773*.
(10) Henglein, A. *J. Phys. Chem. B* **2000**, *104*, 1206.
(11) Giersig, M.; Mulvaney, P. *J. Phys. Chem.* **1993**, *97*, 6334.
(12) Bruchez, M. Jr.; Monroe, M.; Gin, P.; Weiss, S.; Alivisatos, A. P. *Science* **1998**, *281*, 2013.
(13) Shipway, A. N.; Katz, E.; Willner, I. *ChemPhysChem* **2000**, *1*, 18.
(14) El-Sayed, M. A. *Acc. Chem. Res.* **2001**, *34*, 257.
(15) Schroedter, A.; Weller, H.; Eritja, R.; Ford, W. E.; Wessels, J. M. *Nano Lett.* **2002**, *2*, 1363.
(16) Gittins, D. I.; Caruso, F. *Adv. Mater.* **2000**, *12*, 1947.
(17) Gittins, D. I.; Caruso, F. *J. Phys. Chem. B* **2001**, *105*, 6846.
(18) Daniel, M.-C.; Astruc, D. *Chem. Rev.* **2004**, *104*, 293.
(19) Zhao, L.; Kelly, K. L.; Schatz, G. C. *J. Phys. Chem. B* **2003**, *107*, 7343.
(20) Raschke, G.; Brogl, S.; Susha, A. S.; Rogach, A. L.; Klar, T. A.; Feldmann, J.; Fieres, B.; Petkov, N.; Bein, T.; Nichtl, A.; Kürzinger, K. *Nano Lett.* **2004**, *4*, 1853.
(21) Raschke, G.; Kowarik, S.; Franzl, T.; Sönnichsen, C.; Klar, T. A.; Feldmann, J.; Nichtl, A.; Kurzinger, K. *Nano Lett.* **2003**, *3*, 935.
(22) Copland, J. A.; Eghtedari, M.; Popov, V. L.; Kotov, N.; Mamedova, N.; Motamedi, M.; Oraevsky, A. A. *Mol. Imaging Biol.* **2004**, *6*, 341.
(23) Mirkin, C. A.; Letsinger, R. L.; Mucic, R. C.; Storhoff, J. J. *Nature (London)* **1996**, *382*, 607.
(24) Alivisatos, A. P.; Johnsson, K. P.; Peng, X.; Wilson, T. E.; Loweth, C. J.; Bruchez, M. P.; Schultz, P. G. *Nature (London)* **1996**, *382*, 609.
(25) Moskovits, M. *Rev. Mod. Phys.* **1985**, *57*, 783.
(26) Dong, W.-F.; Sukhorukov, G. B.; Möhwald, H. *Phys. Chem. Chem. Phys.* **2003**, *5*, 3003.
(27) Schwartzberg, A. M.; Grant, C. D.; Wolcott, A.; Talley, C. E.; Huser, T. R.; Bogomolni, R.; Zhang, J. Z. *J. Phys. Chem. B* **2004**, *108*, 19191.
(28) Huang, Y.; Duan, X.; Lieber, C. M. *Science* **2001**, *291*, 630.
(29) Kreibig, U.; Vollmer, M. *Optical Properties of Clusters*; Springer-Verlag: Berlin, 1994.
(30) Corbierre, M.; Cameron, N.; Sutton, M.; Mochrie, S. G. J.; Lurio, L. B.; Ruhm, A.; Lennox, R. B. *J. Am. Chem. Soc.* **2001**, *123*, 10411.
(31) Decher, G.; Hong, J. D.; Schmitt, J. *Thin Solid Films* **1992**, *210*, 831.
(32) Lvov, Y.; Decher, G.; Möhwald, H. *Langmuir* **1993**, *9*, 481.
(33) Lvov, Y.; Decher, G.; Haas, H.; Möhwald, H.; Kalachev, A. *Physica B* **1994**, *198*, 89.
(34) Decher, G. *Science* **1997**, *277*, 1232.
(35) Enustun, B. V.; Turkevich, J. *J. Am. Chem. Soc.* **1963**, *85*, *3317*.
(36) Shipway, A. N.; Lahav, M.; Gabai, R.; Willner, I. *Langmuir* **2000**, *16*, 8789.
(37) Westcott, S. L.; Oldenburg, S. J.; Lee, T. R.; Halas, N. J. *Langmuir* **1998**, *14*, 5396.
(38) Zhou, H. S.; Honma, I.; Komiyama, H.; Haus, J. W. *Phys. Rev. B* **1994**, *50*, 12052.
(39) Averitt, R. D.; Sarkar, D.; Halas, N. J. *Phys. Rev. Lett.* **1997**, *78*, 4217.
(40) Oldenburg, S. J.; Averitt, R. D.; Westcott, S. L.; Halas, N. J. *Chem. Phys. Lett.* **1998**, *288*, 243.
(41) Norman, T., Jr.; Grant, C. D.; Magana, D.; Zhang, J. Z.; Liu, J.; Cao, D.; Bridges, F.; van Buuren, A. *J. Phys. Chem. B* **2002**, *106*, 7005.
(42) Norman, T., Jr.; Grant, C. D.; Schwartzberg, A. M.; Zhang, J. Z. *Opt. Mater.* **2005**, *27*, 1197.
(43) Zhang, J. Z.; Schwartzberg, A. M.; Norman, T., Jr.; Grant, C. D.; Liu, J.; Bridges, F.; van Buuren, T. *Nano Lett* **2005**, *5*, 809.

(44) Raschke, G.; Broglk, S.; Susha, A. S.; Rogach, A. L.; Klar, T. A.; Feldmann, J.; Fieres, B.; Petkov, N.; Bein, T.; Nichtl, A.; Kuerzinger, K. *Nano Lett.* **2005**, *5*, 811.
(45) Donath, E.; Sukhorukov, G. B.; Caruso, F.; Davies, S. A.; Möhwald, H. *Angew. Chem., Int. Ed.* **1998**, *37*, 2202.
(46) Skirtach, A. G.; Antipov, A. A.; Shchukin, D. G.; Sukhorukov, G. B. *Langmuir* **2004**, *20*, 6988.
(47) Radt, B.; Smith, T. A.; Caruso, F. *Adv. Mater.* **2004**, *16*, 2184.
(48) Angelatos, A. S.; Radt, B.; Caruso, F. *J. Phys. Chem. B* **2005**, *109*, 3071.
(49) Skirtach, A. G.; Déjugnat C.; Braun, D.; Susha, A. S.; Rogach, A. L.; Parak, W. J.; Möhwald, H.; Sukhorukov, G. B. *Nano Lett.* **2005**, *7*, 1371.
(50) Yuan, X. F.; Fischer, K.; Schartl, W. *Langmuir* **2005**, *21*, 9374.
(51) Déjugnat, C.; Sukhorukov, G. B. *Langmuir* **2004**, *20*, 7265.
(52) Déjugnat, C.; Halozan, D.; Sukhorukov, G. B. *Macromol. Rapid Commun.* **2005**, *26*, 961.
(53) De Geest, B. G.; Déjugnat, C.; Sukhorukov, G. B.; Braeckmans, K.; De Smedt, S. C.; Demeester, J. *Adv. Mater.* **2005**, *17*, 2357.
(54) Skirtach, A. G.; Munoz Javier, A.; Kreft, O.; Köhler, K.; Piera Alberola, A.; Möhwald, H.; Parak, W. J.; Sukhorukov, G. B. *Angew. Chem., Int. Ed.* **2006**, *45*, 4612.
(55) Hiller, S.; Schnackel, A.; Donath, E. *Cytometry Part A* **2005**, *64A*, 119.
(56) Lu, L.; Capek, R.; Kornowski, A.; Gaponik, N.; Eychmüller, A. *Angew. Chem., Int. Ed.* **2005**, *44*, 5997.
(57) Morikawa, M.; Kimizuka, N. *Chem. Commun.* **2005**, *38*, 4866.
(58) Zhang, G.; Wang, D. Y.; Möhwald, H. *Angew. Chem., Int. Ed.* **2005**, *44*, 7767.
(59) Grabar, K. C.; Smith, P. C.; Musick, M. D.; Davis, J. A.; Walter, D. G.; Jackson, M. A.; Guthrie, A. P.; Natan, M. J. *J. Am. Chem. Soc.* **1996**, *118*, 1148.
(60) Giersig, M.; Mulvaney, P. *J. Phys. Chem.* **1993**, *97*, 6334.
(61) Velikov, K. P.; Christova, C. G.; Dullens, R. P. A.; van Blaaderen, A. *Science* **2002**, 296, 5565.
(62) Bhat, R. R.; Genzer, J.; Chaney, B. N.; Sugg, H. W.; Liebmann-Vinson, A. *Nanotechnology* **2003**, *14*, 1145.
(63) Guldi, D. M.; Luo, C. P.; Koktysh, D.; Kotov, N. A.; Da Ros, T.; Bosi, S.; Prato, M. *Nano Lett.* **2002**, *2*, 775.
(64) Petit, C.; Wang, Z. L.; Pileni, M. P. *J. Phys. Chem. B* **2005**, *109*, 15309.
(65) Gittins, D. I.; Caruso F. *Angew. Chem., Int. Ed.* **2001**, *40*, 3001.
(66) Busev, A. I.; Ivanov V. M. *Analiticheskaja khimiya zolota (Analytical chemistry of gold)*; Nauka: Moskva, 1973; pp 28−30 (in Russian).
(67) Samsonov, G. V.; Drozdova S. V. *Sul'fidy (Sulfides)*; Metallurgiya: Moskva, 1972; pp 41−42 (in Russian).
(68) Cölfen, H.; Pauck, T. *Colloid Polym. Sci.* **1997**, *275*, 175.
(69) Cölfen, H.; Pauck, T.; Antonietti, M. *Prog. Colloid Polym. Sci.* **1997**, *107*, 136.
(70) Jain, P. K.; Lee, K. S.; El-Sayed, I. H.; El-Sayed, M. A. *J. Phys. Chem. B* **2006**, *110*, 7238.
(71) Schneider, G.; Decher, G. *Nano Lett.* **2004**, *4*, 1833.
(72) Schneider, G.; Decher, G. *Nano Lett.* **2006**, *6*, 530.
(73) Copland, J. A.; Eghtedari, M.; Popov, V. L.; Kotov, N.; Mamedova, N.; Motamedi, M.; Oraevsky, A. A. *Mol. Imaging Biol.* **2004**, *6*, 341.
(74) Harris, N.; Ford, M. J.; Cortie, M. B. *J. Phys. Chem. B* **2006**, *110*, 10701.
(75) Goldenberg, H.; Tranter, C. J. *Brit. J. Appl. Phys.* **1952**, *3*, 296.
(76) Richardson, H. H.; Hickman, Z. N.; Govorov, A. O.; Thomas, A. C.; Zhang, W.; Kordescht, M. E. *Nano Lett.* **2006**, *6*, 783.
(77) Ge, Z.; Kang, Y.; Taton, T. A.; Braun P. V.; Cahill D. G. *Nano Lett.* **2005**, *5*, 531.
(78) Braun, D.; Libchaber, A. *Phys. Rev. Lett.* **2002**, *89*, 188103.
(79) Arduini, S.; Braun, D. *Eur. Phys. J. E* **2004**, *15*, 277.